RESEARCH

A comprehensive analysis of regional disaggregation coefficients and intensity-duration-frequency curves for the Itacaiúnas watershed in the eastern Brazilian Amazon

Paulo Miguel de Bodas Terassi[1,2] · Paulo Rógenes Monteiro Pontes[3] · Ana Carolina Freitas Xavier[3,4] ·
Rosane Barbosa Lopes Cavalcante[3] · Edivaldo Afonso de Oliveira Serrão[3] · Bruno Serafini Sobral[5] ·
José Francisco de Oliveira-Júnior[6] · Adayana Maria Queiroz de Melo[3] · Jakeline Baratto[1]

Abstract

This study assesses the frequency and intensity of rainfall and determines the optimal methods for estimating extreme rainfall in the Itacaiúnas River watershed (IRW), situated in the eastern Brazilian Amazon. Daily rainfall data from 1988 to 2018 were acquired from the Brazilian National Water Agency (ANA) and the National Institute of Meteorology (INMET), whereas hourly data from 2016 to 2018 were obtained from the Vale Institute of Technology and INMET. To fit the annual maximum daily rainfall data, we employed 11 probability distribution functions (PDFs) and evaluated their efficacy using the Kolmogorov-Smirnov (KS) and Anderson-Darling (AD) tests, as well as the Akaike information criterion (AIC), Bayesian information criterion (BIC), and log-likelihood function (LLF). The Gumbel and gamma distributions yielded superior results, as evidenced by the AIC and BIC criteria. The LLF demonstrated that the GEV and Weibull 3 PDFs better fit the maximum annual rainfall series. We calculated rainfall disaggregation coefficients from the rainfall schedule data to estimate maximum rainfall for different duration periods. A comparison with CETESB coefficients revealed that updating these estimates is necessary for accurately representing intense rainfall events in the eastern Amazon. Our analysis estimated upper hourly maximum rainfall of up to 115 mm/h for a return period of 100 years.

Keywords Return period · Disaggregation coefficients · Probability distribution · IDF curves · Intense rainfall · Hydrology

✉ Paulo Miguel de Bodas Terassi
pmbterassi@gmail.com

Paulo Rógenes Monteiro Pontes
p.rogenes@gmail.com

Ana Carolina Freitas Xavier
anacarolinaf.xavier@gmail.com

Rosane Barbosa Lopes Cavalcante
rosanecavalcante@gmail.com

Edivaldo Afonso de Oliveira Serrão
oliveiraserrao@gmail.com

Bruno Serafini Sobral
brunossobral@gmail.com

José Francisco de Oliveira-Júnior
jose.junior@icat.ufal.br

Adayana Maria Queiroz de Melo
adayana.melo@pq.itv.org

Jakeline Baratto
jakelinebarattogeo@gmail.com

[1] Department of Geography and Postgraduate Program in Physical Geography, University of São Paulo (USP), São Paulo 05508-000, Brazil

[2] Present Address: Vale Institute of Technology – Sustainable Development/Desenvolvimento Sustentável (ITV/DS), Belém, Pará 66055-000, Brazil

[3] Vale Institute of Technology – Sustainable Development/Desenvolvimento Sustentável (ITV/DS), Belém, Pará 66055-000, Brazil

[4] McCoy and Partners, Eindhover, North Brabant, The Netherlands

[5] Land and Cartography Institute of Rio de Janeiro (ITERJ), Rio de Janeiro 20060-060, Brazil

[6] Institute of Atmospheric Sciences, Alagoas Federal University, Maceió, Alagoas 57072-260, Brazil

1 Introduction

Recent changes in the climate may be linked to an increase in the frequency and intensity of extreme precipitation events worldwide, causing socioeconomic losses and environmental impacts (Yilmaz and Perera 2015; Tabari 2020; Fowler et al. 2021; Silva et al. 2021). Such events can exacerbate natural hazards, including landslides and flash floods, in areas with reduced vegetation cover (Merz et al. 2014; Yilmaz et al. 2014; Yilmaz 2017; Dalagnol et al. 2021; Silva Cruz et al. 2022).

In this context, maximum flow analyses are crucial for hydraulic projects such as dam spillways, urban and agricultural drainage, and water-related soil erosion control (Zalina et al. 2002; Cunderlik and Ouarda 2006; Alam et al. 2018; Morabbi et al. 2022). When historical flow data are unavailable, studies of intense rainfall using pluviographic data can provide an alternative. Some of these studies use intensity-duration-frequency (IDF) relationships to estimate rainfall duration on a subdaily scale (usually from 5 to 1440 min) (Beskow et al. 2015; Fadhel et al. 2017; Yilmaz et al. 2017; Costa et al. 2020).

Brazil's lack of subdaily rainfall data poses a significant challenge to designing engineering structures that can mitigate the socioenvironmental impacts of extreme rainfall (Diez-Sierra and del Jesus 2019; Santos et al. 2019a; Santos et al. 2019b; Costa et al. 2020; Lima et al. 2021). Acquiring long subdaily data remains challenging, particularly for field observations in developing countries such as Brazil. To address this issue, rainfall disaggregation methods, such as disaggregation coefficients, are needed to estimate subdaily values from daily data. Disaggregation coefficients, which are based on the relationships observed between hourly rainfall data with varying durations and the annual maximum daily rainfall in a specific area, are widely employed in Brazil due to their straightforward implementation (Koutsoyiannis 2003; Sane et al. 2018; Silva Neto et al. 2017; Abreu et al. 2022).

The use of methodologies, such as disaggregation coefficients, to estimate rainfall at smaller temporal intervals has emerged as a commonly used technique (Caldeira et al. 2015; Martins et al. 2019; Passos et al. 2021). Disaggregation coefficients allow the calculation of precipitation totals based on the characteristics of hourly rainfall rates in a particular region and enable the assessment of the return probability of extreme rainfall events in shorter periods (Pui et al. 2012; Kunkel et al. 2013). Previous studies in Brazil have employed CETESB's disaggregation coefficients (1986), which are averaged from coefficients from several rainfall stations throughout the country; thus, their applicability to specific regions is potentially limited.

The widely used technique for generating IDF curves at subdaily intervals across Brazil is based on the disaggregation coefficients developed by CETESB (1986), as demonstrated in studies by Silveira (2000) for Rio Grande do Sul State, Ferreira et al. (2005) for São Paulo State, Oliveira et al. (2008) for Goiás State, and Passos and Mendes (2018)

for the Balsas Municipality in Maranhão State. However, these coefficients may lead to overestimation or underestimation of maximum hourly rainfall due to their generation throughout Brazil, as reported by Back and Wildner (2021) and Silva Neto et al. (2021). Regional coefficients, however, closely matching local rainfall characteristics, atmospheric dynamics, and associated weather systems are essential.

Thus, this study aimed to analyze the frequency and intensity of extreme rainfall in the Itacaiúnas River basin (IRW) on daily and hourly scales. Additionally, the study evaluated methodological procedures to estimate heavy (R95p) and extreme (R99p) rainfall in greater detail and accuracy. This study uses the nomenclature proposed by Frich et al. (2002), where heavy rainfall is defined as records above 95% of the quantile and extreme rainfall as records that exceed 99% of the quantiles. In addition, the study innovates by adapting the rainfall disaggregation coefficients proposed by CETESB (1986) for Brazil to regional conditions.

The IRW is in the Brazilian Amazon's "Deforestation Arch" in Pará State. Extensive deforestation has occurred since the 1970s, with natural cover replaced by pasture, crop, and mining areas (Souza-Filho et al. 2018; Cavalcante et al. 2019b; Silva Júnior et al. 2019; Silva Júnior et al. 2022; Lima et al. 2022). This intense human intervention in the natural land cover has increased the vulnerability of the IRW to the adverse socioenvironmental effects of extreme rainfall, thereby necessitating further investigation.

This paper's organization is as follows: Section "Materials and methods" presents the study area and the methods used, including data collection, an analysis of homogeneous groups, the probability distribution of extreme rainfall, and IDF based on mean disaggregation coefficients for Brazil and estimated with in situ gauge stations. Section "Results and discussion" presents the results of these analyses, including rainfall regionalization (homogeneous groups), evaluation of FDP fitting to the annual maximum daily rainfall, and comparison of estimates of maximum hourly rain performed by the disaggregation coefficients calculated in this research to those defined by CETESB (1986).

2 Materials and methods

2.1 Study area

The IRW is situated in the southeastern region of Pará in the eastern Brazilian Amazon, covering an area of approximately 41,300 km^2, bounded by latitude 05°10′ to 07°15′S and longitude 48°37′ to 51°25′W (see Fig. 1). It is characterized by the presence of the Serra dos Carajás, a plateau with altitudes ranging between 400 and 900 m, contrasting with the adjacent regions' lower elevations (see Fig. 1A). The Itacaiúnas River is a tributary of the Tocantins River's left bank after the latter's confluence with the Araguaia River (Pontes et al. 2019).
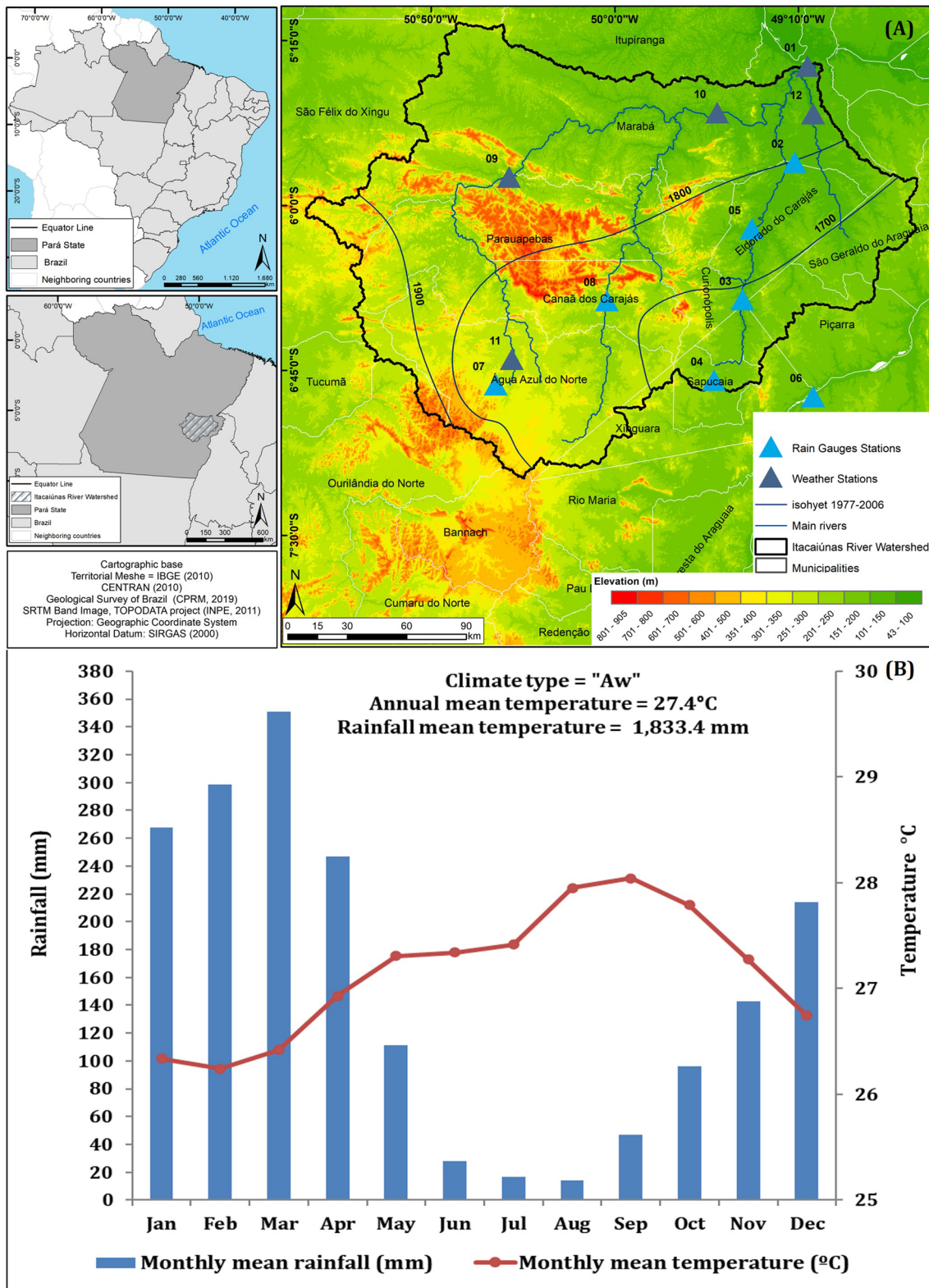
Fig. 1 The geographic location of the Itacaiúnas River watershed (IRW), southeastern Pará State (PA), Brazil, and the spatial distribution of meteorological stations and rainfall stations (in **A**). Climogram for the Marabá (PA) meteorological station from 1976 to 2016 (in **B**)

The basin is primarily used for pasture (51.1%) and mining (0.3%); natural forest covers 48.1% of it, and the remainder is occupied by water bodies (0.3%) and savanna (0.2%) (Nunes et al. 2019). Furthermore, increasing urbanization and industrialization in the cities in the region, especially in Marabá and Parauapebas, two of the largest cities in Pará State (IBGE 2021), have led to a rise in water demand.

The climate of the IRW is classified as "Aw," tropical with a summer rainy season and dry winter, according to the Köppen climate classification (1936) adopted for the Brazilian territory by Álvares et al. (2013). The climate is characterized by humid equatorial conditions with rainfall concentrated primarily in the summer and high temperatures throughout the year. The climogram of the locality of Marabá (PA), used as a reference to characterize the area between 1976 and 2016, shows an average annual temperature of 27.1 °C and average annual rainfall of 1833.4 mm (Fig. 1B). Approximately 83% of the annual rainfall occurs between October and May, which is the rainy season, while from June to September, accumulated rainfall is less than 17% of the annual volume (Tavares et al. 2018; Cavalcante et al. 2019a). The highest rainfall records are observed between December and April, with rainfall totals exceeding 200 mm, contrasting with the period from June to September, with an average rainfall of less than 50 mm. The annual thermal amplitude is low, characteristic of areas near the equator. In Marabá, the thermal averages are above 26 °C for all months of the year, with higher values above 28 °C in the drier months (August and September) and below 27 °C in the wettest months (December and April) (Fig. 1B).

2.2 Methodological procedures

The flowchart in Fig. 2 describes the methodological procedures used, where methodologies differ according to the objective of the analysis and the spatiotemporal availability of hourly and daily data.

2.2.1 Obtaining rainfall data

Daily rainfall data were collected from six Brazilian National Water Agency (ANA 2021) stations and one conventional meteorological station of the Brazilian National Institute of Meteorology (INMET 2021), covering the period 1988 to 2018. The data had a maximum of 10.58% missing values (station ID 02—Eldorado dos Carajás) and a minimum of 0.13% (station ID 01—Marabá). Missing data were filled in using the PERSIANN-CDR satellite product, following the recommendations of Xavier et al. (2021) for the Mearim River basin. In addition, complete hourly rainfall data during the selected period for 2016 to 2018 were obtained from weather stations managed by the Vale Institute of Technology (ITV 2021) and the Marabá (INMET) station.

2.2.2 Cluster analysis for identifying the homogeneous rainfall groups

The study employed a clustering technique to identify homogeneous rainfall groups in the IRW. The squared Euclidean distance, which measures the geometric distance between two observations in multidimensional space, was used as a proximity measure. The Ward method (Ward 1963) was applied to daily data series to group meteorological and rainfall stations with similar rainfall characteristics. The dendrogram was generated using Statistica 10 software. The physiographic factors, such as relief, rainfall regime, and proximity space between the rainfall stations, were used to delimit homogeneous groups, a technique used in previous studies (Teodoro et al. 2016; Shiau and Lin 2016; Terassi et al. 2020; Brasil Neto et al. 2021; Zerouali et al. 2022).
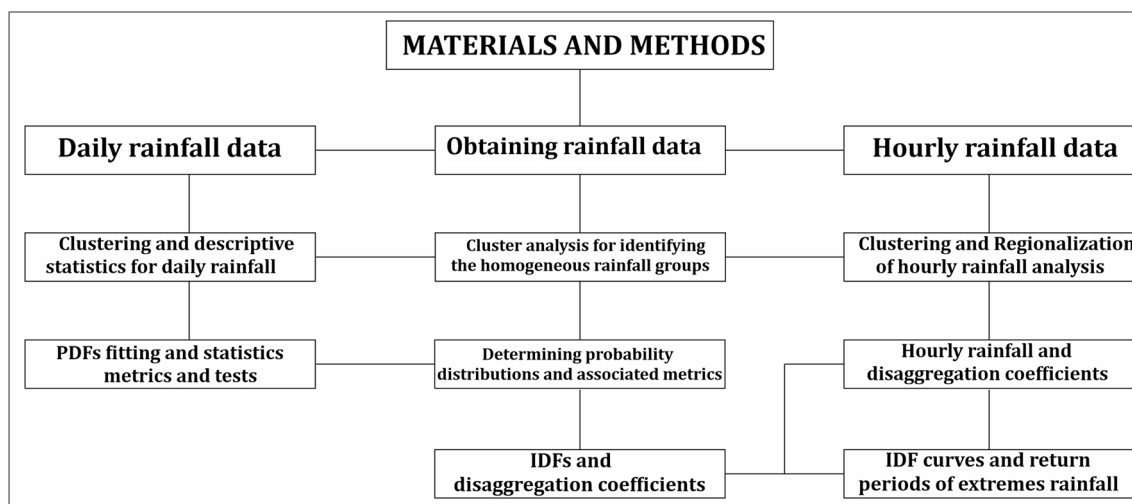
Fig. 2 Flow chart for methodological procedures applied for extreme rainfall analysis in the IRW

Descriptive statistics were computed to determine the maximum value, lower quartile (LQ), higher quartile (HQ), outliers, and percentiles (95th and 99th) of the data set (Yang et al. 2017). Outliers were identified using Eq. 1, which involves adding 1.5 times the interquartile range (HQ-LQ) to the average of the daily rainfall.

$$Outlier = average + 1.5\ (HQ - LQ) \tag{1}$$

The nomenclature suggested by Frich et al. (2002) was adopted to define heavy rainfall, using the acronym R95p for daily records equal to or greater than the 95th quantile and R99p for intense daily rainfall equal to or greater than the 99th quantile.

2.2.3 Determining probability distributions and associated metrics

Annual maximum daily rainfall data for the period 1988–2018 from the ANA and INMET meteorological stations were fitted to 11 probability distribution functions (PDFs): Fréchet, gamma, gamma 3 parameters, generalized extreme value (GEV), Gumbel, log gamma 3 parameters, log-normal, log normal 3 parameters, normal, Weibull, and Weibull 3 parameters. These PDFs are widely used in the literature for maximum daily rainfall estimation in various regions (Koutsoyiannis et al. 1998; Katz 2010; Rulfová et al. 2016; Yuan et al. 2018; Xavier et al. 2019a; Lima et al. 2021).

The Kolmogorov-Smirnov (KS) and Anderson-Darling (AD) tests were employed to assess the goodness of fit of each PDF (Fischer et al. 2012; Ye et al. 2018; Xavier et al. 2019b; Moccia et al. 2021). The Akaike information criterion (AIC), Bayesian information criterion (BIC), and log-likelihood function (LLF) validation metrics were used to compare and select the best-fitting PDF (Coles

and Dixon 1999; Svensson et al. 2007; Svensson and Jones 2010). The PDFs with the lowest AIC and BIC values were considered to best describe and model the maximum daily annual rainfall estimates. The Friedman nonparametric test was utilized to categorize the PDFs based on their ordering within a categorized set (Cahill 2003; Kim et al. 2017; Navares and Aznarte 2020).

$$AIC = -2loglog\ (ML) + 2k \tag{2}$$

$$BIC = -2log\ (ML) + klog\ (n) \tag{3}$$

where log (ML) is the maximized log-likelihood function under the proposed model and k is the number of parameters in a given model.

2.2.4 IDFs and disaggregation coefficients

IDF curves are a widely used tool in hydraulic engineering for estimating the "project design rainfall," a hypothetical rainfall event used to design hydraulic structures based on the maximum daily rainfall records. This study calculated disaggregation coefficients for ITV and INMET meteorological stations using the hourly rainfall average and its proportional relationship to other hourly intervals (01, 06, 08, 10, and 12 h). Table 1

The frequency of a rainfall event is commonly associated with its return period (RP), which represents the time interval in which a rainfall value can be equal to or exceeded (Papalexiou et al. 2013). The longer the RP of a precipitation value is, the lower the probability of that event being equaled or surpassed, whereas the shorter the RP is, the greater the probability of rainfall being equaled or exceeded. This concept has been well established in the literature (Mohymont et al. 2004; Ghiaei et al. 2018).

Table 1 Identification (ID), geographic location (latitude and longitude), altitude, analysis period, and data record failures (%) of the rainfall stations and meteorological stations* located on the IRW and its surroundings

ID	Municipality	Lat. (°)	Long. (°)	Altitude (m)	Period	Faults (%)	Annual average rainfall (mm)
01*	*Marabá*	− 5.366	− 49.125	95.0	1988–2018	0.13	1845.3
02	*Eldorado dos Carajás*	− 5.803	− 49.183	131.0	1988–2018	10.58	1716.7
03	*Eldorado dos Carajás*	− 6.428	− 49.420	137.0	1988–2018	4.45	1659.2
04	*Sapucaia*	− 6.795	− 49.549	191.0	1988–2018	1.61	1488.3
05	*Eldorado dos Carajás*	− 6.105	− 49.378	141.0	1988–2018	5.85	1918.1
06	*Xinguara*	− 6.869	− 49.099	157.0	1988–2018	5.87	1588.9
07	*Água Azul do Norte*	− 6.815	− 50.539	303.0	1988–2018	7.53	1529.5
08*	*Canaã dos Carajás*	− 6.443	− 50.035	236.0	2016–2018	0.00	1220.7
09*	*Marabá*	− 5.871	− 50.479	178.0	2016–2018	0.00	1660.5
10*	*Marabá*	− 5.578	− 49.535	134.0	2016–2018	0.00	1723.9
11*	*Água Azul do Norte*	− 6.699	− 50.466	259.0	2016–2018	0.00	1554.1
12*	*Marabá*	− 5.825	− 49.099	111.0	2016–2018	0.00	1812.1

The creation of the IDF curves followed these steps:

i   Definition of annual daily maximums for the conventional (ITV and INMET) data series (1988 to 2018)
ii Determination of the maximum daily rainfall for the RPs (2, 5, 10, 25, 50, and 100 years) according to the 11 probability distributions (Section "Determining probability distributions and associated metrics")
iii Delimitation of homogeneous groups of daily rainfall considering the 12 meteorological stations (INMET)
iv Calculation of the disaggregation coefficients from the hourly rainfall of the network of ITV and INMET stations (Table 2)
v   Disaggregation of maximum daily rainfall from the disaggregation coefficients of CETESB (1986) and calculated by the present research
vi Generation of IDF (mm/h) curves from the disaggregation coefficients calculated by the hourly data acquired from the ITV and INMET meteorological stations

The study estimated the disaggregation coefficients of rainfall intensity for two meteorological stations (ITV and INMET) and compared them with the mean values for Brazil (CETESB) across different hourly durations (1 h, 6 h, 8 h, 10 h, and 12 h) out of 24 h. The coefficients were calculated by evaluating the direct proportionality between the maximum hourly rainfall and the maximum daily rainfall at the selected stations. Although subhourly coefficients were available for CETESB, hourly time steps of ITV and INMET stations limited their estimation for the IRW.

3 Results and discussion

3.1 Analysis of homogeneous groups and rainfall intensity

3.1.1 Daily rainfall characterization and cluster analysis

Cluster analysis revealed the presence of two homogeneous groups (HGs) that differed primarily from December to May

Table 2 Disaggregation coefficients for the homogeneous groups (HGs) in the IRW, calculated for Brazil (CETESB 1986)

Relation	CETESB (1986)	HG-I	HG-II	HG-III	HG-IV
1 h/24 h	0.420	0.530	0.321	0.375	0.414
6 h/24 h	0.720	0.750	0.593	0.582	0.648
8 h/24 h	0.780	0.828	0.496	0.632	0.724
10 h/24 h	0.820	0.824	0.779	0.902	0.754
12 h/24 h	0.850	0.851	0.877	0.893	0.830

(Fig. 3). The monthly averages in HG-I were greater than 300 mm in February (313 mm) and March (333.9 mm), while HG-II reported a maximum of 247.4 and 257.7 mm during these same months. The average annual rainfall was estimated at 1826.7 mm and 1559.0 mm for HG-I and HG-II, respectively.

The analysis of daily rainfall data showed that HG-I exhibited higher levels of heavy (R95p) and intense (R99p) rainfall between February and March, with thresholds greater than 40 mm and 70 mm in December, respectively. The maximum daily rainfall for HG-I was recorded in October (225.3 mm), December (182.0 mm), and April (175.3 mm), with rainfall above 150 mm typically observed from October to December, February, April, and May. Outliers were detected between January and April, with values exceeding 20 mm and a maximum above 30 mm between February and March (Table 3).

For HG-II, heavy and intense rains were also identified between February and March, with R95p thresholds greater than 40 mm and R99p records exceeding 70 mm in December. The maximum daily values were observed between December and May (> 140 mm), especially in January (170.0 mm) and April (165.5 mm). Outliers exceeding 15 mm were detected between January and April, with the maximum in February (23.6 mm) and March (23.3 mm) (Table 3).

The rainfall regime in the studied region is mainly influenced by the southern position of the Intertropical Convergence Zone (ITCZ) during the Southern Hemisphere summer and the South Atlantic Convergence Zone (SACZ), which generates rainfall (Nobre et al. 1991; Marengo 2005). Variability in the convection center of the Lower Amazon (Hastenrath and Geischar 1993; Carvalho et al. 2002) also impacts rainfall amounts. The role of frontal systems in organizing mesoscale convective systems that produce abundant rainfall, particularly in the rainy season, is noteworthy (Falck et al. 2015; Serrão et al. 2021). Instability lines, which usually form along Brazil's northern coast and propagate inland every 2 days, are also significant, with more or less frequency between April (October) and June (November) (Cohen et al. 1995; Alcântara et al. 2011; Almeida et al. 2017).

3.1.2 Hourly rainfall characterization and cluster analysis

The cluster analysis conducted on hourly rainfall data in the IRW identified four HGs (Fig. 4), which differed from the grouping obtained with daily rainfall data. These differences were more pronounced between the wet and dry months. The clustering was critical in establishing and adapting the disaggregation coefficients, which were then applied to the daily time series between 1988 and 2018.

HG-I represents the wettest sector of the IRW, in the E and NE, with an average annual rainfall of 1877.2 mm. HG-II, situated in the central and SE sectors, has an average annual rainfall of 1238.9 mm. HG-IV, in the N and
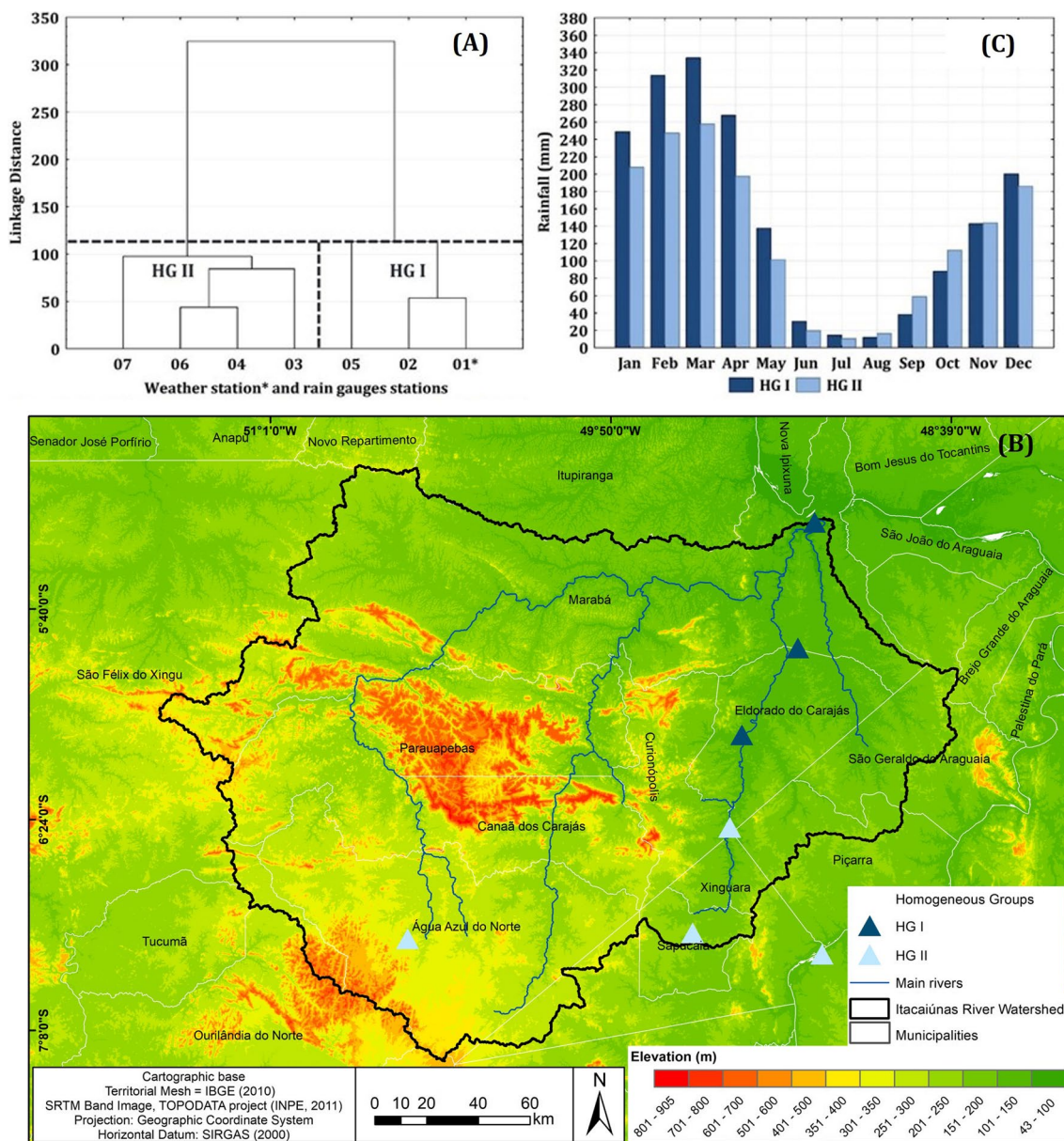
Fig. 3 Dendrogram (Ward's method—in **A**) and the spatial distribution of homogeneous groups (HGs) and hypsometry (m) for daily rainfall in the IRW (in **B**). Monthly rainfall distribution (mm) in homogeneous groups (HGs) of the IRW (in **C**), according to daily records (1988–2018)

NE sectors of the IRW, has an average annual rainfall of 1587.2 mm. In contrast, HG-III, found in the W and SE sectors of the watershed, has an average annual rainfall of 1554.0 mm (Fig. 4).

From November to April, HG-I exhibits average monthly rainfall exceeding 200 mm and reaching values above 300 mm in February and March. HG-II and HG-III have average monthly rainfall exceeding 200 mm between January and March, with HG-III having maximum rainfall exceeding 300 mm between February and March. During the rainy season, HG-II has significantly lower averages than the other homogeneous groups, with values below 150 mm between November

and January and higher rainfall between February and March (> 200 mm). The driest period is from June to September, with averages below 60 mm, and in July, the average rainfall does not exceed 10 mm in any homogeneous group (Fig. 4).

3.2 Probability distributions, IDF curves, and return periods

3.2.1 Probability distributions of heavy and intense rainfall

The observed data adjustments generated by the PDFs were ineffective based on the results of the KS and AD tests. For

Table 3 Descriptive daily rainfall (mm) statistics for HG-I and HG-II in the IRW

GH-I	Maximum	Lower quartile	Upper quartile	Outliers	Percentile 95 (R95p)	Percentile 99 (R99p)
January	130.6	0.0	10.4	23.8	38.4	64.3
February	150.3	0.0	14.6	33.1	48.5	76.0
March	130.8	0.0	15.5	34.2	44.9	74.1
April	175.3	0.0	11.3	25.9	41.1	73.4
May	163.2	0.0	3.2	9.3	27.2	55.9
June	119.1	0.0	0.0	1.0	5.3	21.4
July	55.8	0.0	0.0	0.5	1.0	14.3
August	53.7	0.0	0.0	0.4	0.1	11.3
September	120.0	0.0	0.0	1.3	9.15	26.8
October	225.3	0.0	0.1	3.1	18.5	47.1
November	162.8	0.0	2.0	7.8	30.3	58.2
December	182.0	0.0	6.5	16.3	33.6	72.3
GH-II	Maximum	Lower quartile	Upper quartile	Outliers	Percentile 95 (R95p)	Percentile 99 (R99p)
January	170.0	0.0	7.3	17.7	34.8	67.0
February	151.9	0.0	9.9	23.6	43.3	76.6
March	144.2	0.0	9.9	23.3	40.2	70.6
April	165.5	0.0	7.1	17.3	34.7	67.1
May	140.0	0.0	0.6	4.2	20.1	51.0
June	99.0	0.0	0.0	0.7	2.4	19.0
July	93.0	0.0	0.0	0.3	0.0	10.0
August	70.0	0.0	0.0	0.5	0.7	17.4
September	145.7	0.0	0.0	2.0	12.9	37.8
October	162.2	0.0	0.0	3.7	23.5	56.0
November	128.1	0.0	2.4	8.4	30.6	61.3
December	113.0	0.0	5.2	13.8	35.5	71.6

ID03 (HG-II) station values, more robust adjustments were identified for PDFs gamma 3, normal, and Weibull (95% significance), while gamma and log-normal presented 90% significance (Tables 4 and 5 - Fig. S1). AIC values lower than 300 were identified for all PDFs in ID 01, ID 06, and ID 03, except for Fréchet and log gamma 3 in the latter. BIC values lower than 300 were obtained for all PDFs in ID 06, except for Weibull in ID 01. The log-likelihood function indicated values lower than − 145 in all ID 06 (HG-II) PDFs and, except for normal and Weibull, in ID 01 (HG-I). However, none of the PDFs showed goodness of fit for the observed data in ID 06 (HG-I), ID 04 (HG-II), and ID 07 (HG-II) when considering all the metrics and tests described above (Tables 4 and 5—Fig. S2).

The use of PDFs for analyzing historical heavy and intense daily rainfall series indicated that the Fréchet distribution had the highest values, ranging from 140.1 to 162 mm for R95p and 179.1 to 219.7 mm for R99p. However, the Gumbel PDF produced the highest values in ID 02, with 173.2 mm for R95p and 221.0 mm for R99p. In contrast, the normal distribution yielded the lowest values for R95p

and intense R99p rains at most rainfall stations, ranging between 121.9 and 154.3 mm and 147.9 and 176.2 mm, respectively (Tables 4 and 5 - Fig. S3). The KS and AD tests revealed that the PDFs had better performance in ID 02 and ID 06, while poorer performances were observed in ID 04 and ID 05 for the KS test and in ID 01 and ID 02 for the AD test (Fig. S1).

The AIC metric indicated that the Gumbel (300.8) and gamma (301.1) probability density functions (PDFs) had better fits to the time series of annual maximum daily rainfall. In contrast, the BIC metric revealed that the Gumbel (303.6) and gamma (303.9) PDFs provided better adjustments. The Weibull (304.4) and normal (303.9) PDFs had lower adjustments for the AIC metric, while the Log gamma 3 (307.4) and Weibull (307.3) distributions produced the worst results for the BIC metric (Table 6 - Fig. S2).

The log-likelihood function revealed that GEV (− 147.6), Weibull 3 (− 147.6), log-normal 3 (− 147.7), and gamma 3 (− 147.9) are the most suitable PDFs for estimating the maximum annual rainfall in the IRW. However, the Weibull (− 150.2) and normal (− 150.0) PDFs showed the greatest
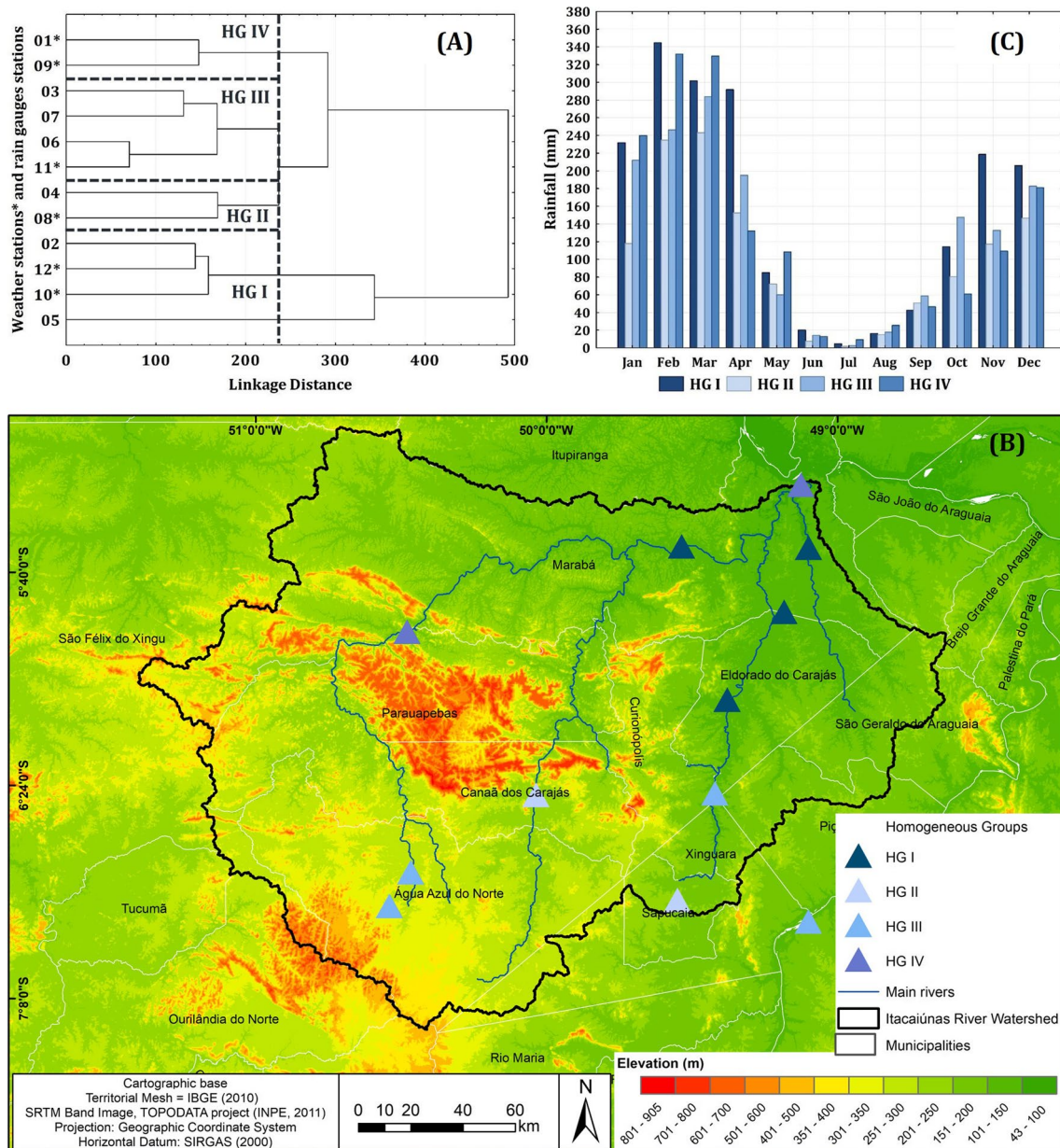
Fig. 4 Dendrogram (Ward's method—in **A**) and the spatial distribution of the homogeneous groups (HGs) and hypsometry (m) for hourly rainfall in the IRW (in **B**). Monthly rainfall distribution (mm) in homogeneous groups (HGs) in the IRW (in **C**), according to hourly rainfall records (2016–2018)

misfits and are thus not recommended for use in the IRW (Table 6 - Fig. S2).

The Gumbel and gamma distributions better fit the maximum annual rainfall series in the IRW, as indicated by the metrics. However, the GEV and Weibull 3 PDFs best fit according to the log-likelihood function. The normal and Weibull PDFs significantly underestimated the intense rains in the IRW, and they showed the worst adjustments to the annual maximum daily rainfall in the IRW in all the evaluated metrics.

Beskow et al. (2015) conducted a study on *Rio Grande do Sul* in southern Brazil and identified the kappa probability distribution as the most appropriate for estimating maximum rainfall, with GEV and Gumbel distributions also suitable. Blain et al. (2021) investigated maximum annual rainfall data for the state of São Paulo in southern Brazil and found that the GEV and generalized logistic distributions (GLOs) accurately modeled annual maximum daily rainfall. Similarly, Lima et al. (2021) indicated that the Gumbel, GEV, and log-normal distributions were suitable for representing

Table 4 Descriptive level (*p* value) for the Kolmogorov-Smirnov (KS) and Anderson-Darling (AD) test, log-likelihood (loglik), Akaike information criteria (AIC), Bayesian information criteria (BIC), and estimated annual daily rainfall intensity for 95 (R95p) and 99 percentiles (R99p) for probability distribution functions to estimate the maximum daily rainfall at rain gauges and the weather station for HG-I in the IRW, eastern Amazon, Brazil

Distribution	ID	*p* value (KS)	*p* value (AD)	loglik	AIC	BIC	R95p	R99p
Fréchet	01	0.95	0.98	**− 143.9**	**293.8**	**298.1**	158.4	193.8
Gamma	01	0.73	0.87	**− 144.4**	**292.7**	**295.6**	152.2	175.8
Gamma 3	01	0.88	0.95	**− 144.0**	**294.0**	**298.3**	155.0	182.8
GEV	01	0.94	0.98	**− 143.8**	**293.7**	**298.0**	155.7	186.6
Gumbel	01	0.96	0.98	**− 143.9**	**291.8**	**294.6**	158.0	193.3
Log Gamma 3	01	0.92	0.97	**− 143.9**	**293.8**	**298.1**	155.3	186.3
Log Normal 3	01	0.86	0.95	**− 144.0**	**293.9**	**298.2**	154.0	181.9
Log Normal	01	0.87	0.95	**− 144.0**	**291.9**	**294.8**	153.9	181.8
Normal	01	0.43	0.54	− 146.1	**296.2**	**299.1**	150.4	168.8
Weibull	01	0.35	0.39	− 147.2	**298.5**	301.3	153.6	171.1
Weibull 3	01	0.77	0.84	**− 144.4**	**294.7**	**299.0**	155.2	179.2
Fréchet	02	0.92	0.82	− 147.2	300.3	304.5	172.2	219.5
Gamma	02	0.81	0.85	− 146.6	**297.2**	300.0	161.7	194.4
Gamma 3	02	0.64	0.82	− 146.3	**298.5**	302.7	157.6	185.1
GEV	02	0.64	0.82	− 146.1	**298.3**	302.5	157.1	181.2
Gumbel	02	0.90	0.82	− 147.2	**298.3**	301.1	173.2	221.0
Log Gamma 3	02	0.95	0.77	− 147.8	301.6	305.8	170.7	217.9
Log Normal 3	02	0.64	0.83	− 146.2	**298.5**	302.7	157.7	185.7
Log Normal	02	0.95	0.79	− 147.6	**299.2**	302.0	169.5	214.4
Normal	02	0.42	0.69	− 146.6	**297.3**	300.1	154.3	176.2
Weibull	02	0.45	0.70	− 146.7	**297.3**	300.2	155.9	176.8
Weibull 3	02	0.55	0.75	− 146.5	**299.0**	303.2	156.7	179.4
Fréchet	05	0.90	0.88	− 149.9	305.9	310.3	145.1	199.6
Gamma	05	0.94	0.80	− 152.1	308.2	311.1	138.1	167.3
Gamma 3	05	0.44	0.39	− 148.9	303.8	308.2	158.1	216.8
GEV	05	0.90	0.87	− 149.9	305.9	310.3	145.9	202.3
Gumbel	05	0.97	0.91	− 150.5	305.1	308.0	137.3	173.4
Log Gamma 3	05	0.90	0.85	− 149.8	305.6	310.0	147.0	203.4
Log Normal 3	05	0.92	0.84	− 149.8	305.5	309.9	147.6	201.7
Log Normal	05	0.97	0.91	− 150.6	305.3	308.2	138.9	174.5
Normal	05	0.69	0.30	− 157.4	318.9	321.8	139.6	162.2
Weibull	05	0.49	0.25	− 156.6	317.2	320.1	146.7	173.5
Weibull 3	05	0.71	0.58	− 148.7	303.4	307.8	153.1	202.8

Legend: * = 95% significance; The expressive metrics are highlighted in bold

annual maximum daily rainfall in *Rio de Janeiro* in southern Brazil; similar results were obtained in this research.

Abreu et al. (2018) conducted statistical tests using KS and AD to evaluate extreme daily rainfall in the southwest region of *Minas Gerais* (southern Brazil). They found that the Gumbel and GEV probability distributions were better suited for estimating rainfall extremes in this area. In the Brazilian Amazon, Santos et al. (2015) showed that the GEV and Pareto distributions had a good fit for estimating seasonal maximum daily rainfall in different subbasins, with the GEV distribution being the most suitable. In the southeast region of Pará, where the IRW is located, the Gumbel distribution estimated maximum daily rainfall values between 106.5 and 299.6 mm during the austral autumn (March to May).

Ximenes et al. (2021) analyzed the monthly average rainfall series for the Brazilian northeast region (NEB) and found that the gamma and Weibull distributions fit well. The log-normal and generalized Pareto distributions also presented satisfactory results in some regions and certain months. However, these results differ from the estimates of maximum daily rainfall for the IRW.

3.2.2 IDF curves and return periods of extreme rainfall

A comparison of the disaggregation coefficients showed that CETESB's values from 1986 underestimated hourly rainfall at HG-I compared to those obtained in this study. The maximum rainfall intensity for a 100-year return

Table 5 Descriptive level (*p* value) for the Kolmogorov-Smirnov (KS) and Anderson-Darling (AD) test, log-likelihood (LLK), Akaike information criteria (AIC), Bayesian information criteria (BIC), and estimated annual daily rainfall intensity for 95 (R95p) and 99 percentiles (R99p) for probability distribution functions to estimate the maximum daily rainfall at rain gauges and the weather station for HG-II in the IRW, eastern Amazon, Brazil

Distribution	ID	*p* value (KS)	*p* value (AD)	LLK	AIC	BIC	R95p	R99p
Fréchet	03	0.40	0.81	− 148.5	303.0	307.4	162.8	219.7
Gamma	03	0.06+	0.30	− 150.7	305.4	308.3	152.8	178.3
Gamma 3	03	0.04*	0.25	− 151.5	308.9	313.3	153.3	177.4
GEV	03	0.40	0.81	− 148.5	303.0	307.4	162.6	219.4
Gumbel	03	0.21	0.55	− 149.0	302.1	305.0	153.0	187.1
Log Gamma 3	03	0.36	0.80	− 148.4	302.9	307.3	162.5	213.8
Log Normal 3	03	0.35	0.79	− 148.4	302.8	307.2	162.1	210.3
Log Normal	03	0.10+	0.42	− 149.8	303.7	306.6	153.9	183.8
Normal	03	0.02*	0.15	− 153.2	310.4	313.3	151.6	171.4
Weibull	03	0.02*	0.15	− 153.8	311.7	314.6	154.8	174.0
Weibull 3	03	0.21	0.64	− 148.4	302.8	307.2	159.4	192.0
Fréchet	04	0.73	0.70	− 150.6	307.2	311.6	155.3	199.6
Gamma	04	0.93	0.87	− 149.6	303.3	306.2	142.2	167.3
Gamma 3	04	0.96	0.87	− 149.6	305.2	309.6	141.3	165.3
GEV	04	0.95	0.87	− 149.6	305.2	309.6	141.8	164.6
Gumbel	04	0.77	0.77	− 150.3	304.5	307.5	151.6	190.0
Log Gamma 3	04	0.72	0.75	− 150.3	306.6	311.0	148.9	185.3
Log Normal 3	04	0.80	0.81	− 150.0	306.0	310.4	146.1	178.1
Log Normal	04	0.80	0.81	− 150.0	304.0	306.9	146.0	177.9
Normal	04	0.88	0.73	− 150.3	304.7	307.6	138.1	156.2
Weibull	04	0.75	0.61	− 150.8	305.6	308.5	139.8	156.8
Weibull 3	04	0.90	0.78	− 149.7	305.4	309.8	141.6	162.9
Fréchet	06	0.19	0.29	**− 143.8**	**293.6**	**298.0**	140.1	179.1
Gamma	06	0.37	0.48	**− 141.7**	**287.5**	**290.4**	125.0	143.6
Gamma 3	06	0.51	0.55	**− 141.6**	**289.1**	**293.5**	123.1	139.0
GEV	06	0.48	0.52	**− 141.7**	**289.4**	**293.8**	124.3	139.2
Gumbel	06	0.22	0.34	**− 143.1**	**290.2**	**293.1**	135.2	166.2
Log Gamma 3	06	0.25	0.39	**− 142.3**	**290.6**	**295.0**	128.4	152.1
Log Normal 3	06	0.52	0.55	**− 141.6**	**289.1**	**293.5**	123.1	139.0
Log Normal	06	0.27	0.40	**− 142.2**	**288.4**	**291.3**	127.6	150.2
Normal	06	0.65	0.58	**− 141.7**	**287.4**	**290.3**	121.9	135.7
Weibull	06	0.60	0.52	**− 142.4**	**288.8**	**291.7**	122.3	134.1
Weibull 3	06	0.48	0.53	**− 141.5**	**289.0**	**293.4**	123.4	138.0
Fréchet	07	0.84	0.78	− 154.8	315.6	320.0	141.8	185.0
Gamma	07	0.89	0.80	− 154.7	313.3	316.2	137.4	171.8
Gamma 3	07	0.85	0.87	− 153.9	313.8	318.2	130.7	156.8
GEV	07	0.82	0.86	− 153.8	313.6	318.0	130.0	152.6
Gumbel	07	0.88	0.80	− 154.8	313.5	316.5	144.2	188.5
Log Gamma 3	07	0.57	0.52	− 156.9	319.8	324.2	152.9	211.2
Log Normal 3	07	0.85	0.88	− 153.9	313.8	318.2	130.7	157.3
Log Normal	07	0.62	0.57	− 156.6	317.2	320.2	150.3	204.6
Normal	07	0.68	0.75	− 154.3	312.6	315.6	127.4	147.9
Weibull	07	0.71	0.80	− 154.0	312.0	314.9	129.9	151.6
Weibull 3	07	0.73	0.81	− 154.0	314.0	318.3	130.1	152.2

Legend: * = 95% significance; + = 90% significance. The expressive metrics are highlighted in bold

period event in 60 min was 125.0 mm/h using the coefficient established in this research, while it was 117.6 mm/h using CETESB's (1986) coefficient in ID 02. This pattern of underestimation is consistent across different rainfall durations (Fig. 5). In contrast, for HG-II and IV, CETESB's (1986) coefficients overestimate the intensity

Table 6 The mean value for each metric related to the model's goodness of fit (loglik, AIC, and BIC) and the corresponding compact letter display of the Friedman multiple comparison post hoc tests at a 5% significance level. According to the Friedman test, the metrics for distributions followed by the same letter are not different

Distribution	LLK (mean)	LLK (sd)	cld	AIC	AIC (sd)	cld	BIC	BIC (sd)	cld
Fréchet	− 148.4	3.90	abc	302.8	7.80	a	307.1	7.82	a
Gamma	− 148.5	4.53	abc	301.1	9.07	a	303.9	9.08	ab
Gamma 3	− 147.9	4.30	abc	302.0	8.59	a	306.3	8.62	ab
GEV	− 147.6	4.07	a	301.3	8.16	a	305.6	8.18	ab
Gumbel	− 148.4	4.07	abc	300.8	8.14	a	303.6	8.15	b
Log Gamma 3	− 148.5	4.75	abc	303.0	9.51	a	307.4	9.52	a
Log Normal 3	− 147.7	4.75	ab	301.3	8.25	a	305.7	8.27	ab
Log Normal	− 148.7	4.74	abc	301.4	9.50	a	304.2	9.51	ab
Normal	− 150.0	5.47	bc	303.9	10.94	a	306.8	11.0	ab
Weibull	− 150.2	5.01	c	304.4	10.02	a	307.3	10.1	a
Weibull 3	− 147.6	3.99	ab	301.2	7.99	a	305.5	8.01	ab

of estimated rains for various durations and return periods. The differences between the rainfall intensity values generated by the two methodologies were smaller in HG-IV than in HG-II. The results demonstrate that the application of CETESB's (1986) DC overestimates the rainfall intensity of different durations and return periods in this sector of the IRW. For HG-III, the maximum estimated rainfall lasting 60, 360, 480, and 1440 min had higher intensity than CETESB's (1986) DC, while the maximum rain lasting 720 and 600 min was more intense in CETESB (1986) than in the DC proposed in this study (Fig. 5).

The study area's adapted coefficients yielded maximum rainfall intensities of 125.0 and 117.6 mm/h for a 100-year RP in ID 02 and ID 05 (HG-I), respectively, while ID 06 and ID 04 had the lowest rainfall intensity values of 63.1 and 64.7 mm/h, respectively, for the same duration (Table 7). The ID 02 rainfall station (HG-I) recorded the highest rainfall intensity totals for 1440 min, with values ranging between 7.7 and 9.8 mm/h for RPs equal to or greater than 25 years, whereas for RPs of 2 to 10 years, ID 01 (HG-IV) exhibited the highest daily rainfall, ranging from 4.0 to 6.2 mm/h (Table 7).

For RPs equal to or greater than 10 years, ID 06 (HG-III) is expected to have less intense rainfall intensities, ranging from 4.9 to 7.0 mm/h over 1440 min. Consequently, the expected 1440-min rainfall intensity for a 100-year RP in ID 02 (9.8 mm/h) is 40% greater than that estimated for ID 06 (7.0 mm/h). The lowest 1440-min intensities for RPs of 2 and 5 years are anticipated at ID 07 (HG-III), with values of 2.9 mm/h and 4.2 mm/h, respectively (Table 7).

Silva Neto et al. (2020) analyzed the state of Tocantins and reported rainfall intensities lasting 1440 min ranging from 7 mm/h (RP10y) to 12 mm/h (100-year RP). For rainfall durations of 720 min, the intensities were 14, 20, and 23 mm/h for RPs equal to 10, 50, and 100 years, respectively. The extreme N and NW regions of Tocantins, adjacent to the IRW, experienced the highest intense rainfall due to the prevalence of the Continental Equatorial air mass,

which facilitates convective rainfall of short duration and high intensity. Santos et al. (2015) identified the Brazilian Amazon as the rainiest region in Brazil, with a maximum daily intensity estimated to be between 219.5 mm (west) and 430.5 mm (east) for a 100-year RP.

4 Conclusions

The IRW sectors with the highest rainfall totals were identified through cluster analysis. HG-I in the SE and NE watershed sectors had the highest rainfall, followed by HG-II in the S and SW sectors. Rainfall is concentrated (> 90%) in both homogeneous rainfall groups from October to May, with the highest totals in February and March. HG-I (February to April) experienced the most intense daily rainfall for the thresholds of R95p and R99p. The statistical tests and metrics indicated that the rainfall time series adhered well to the PDFs. The Gumbel and gamma distributions fit more closely to the series of maximum annual rainfall in the IRW, as indicated by the AIC and BIC metrics. The LLF indicated the best fit for the GEV and Weibull 3 PDFs. The normal and Weibull distributions mostly underestimated the intense rains in the IRW, as the PDFs were less adjusted to the IRW rain time series.

Calculating disaggregation coefficients as a function of homogeneous groups and patterns allows for evaluating and estimating rainfall totals at other stations by adapting to the dynamics of regional rainfall. However, CETESB's disaggregation coefficients (CETESB 1986) underestimate the maximum hourly rainfall for HG-I and overestimate the maximum rainfall for HG-II and IV for different RPs. IDF curves demonstrate values exceeding 115.0 mm/h for a maximum rainfall of 60 min and RP of 100 years in HG-I. Conversely, the lowest value (~ 65 mm/h) for maximum hourly rainfall for the RP of 100 years was recorded in HG-II. This study is expected to contribute to redimensioning agricultural, urban, and road drainage
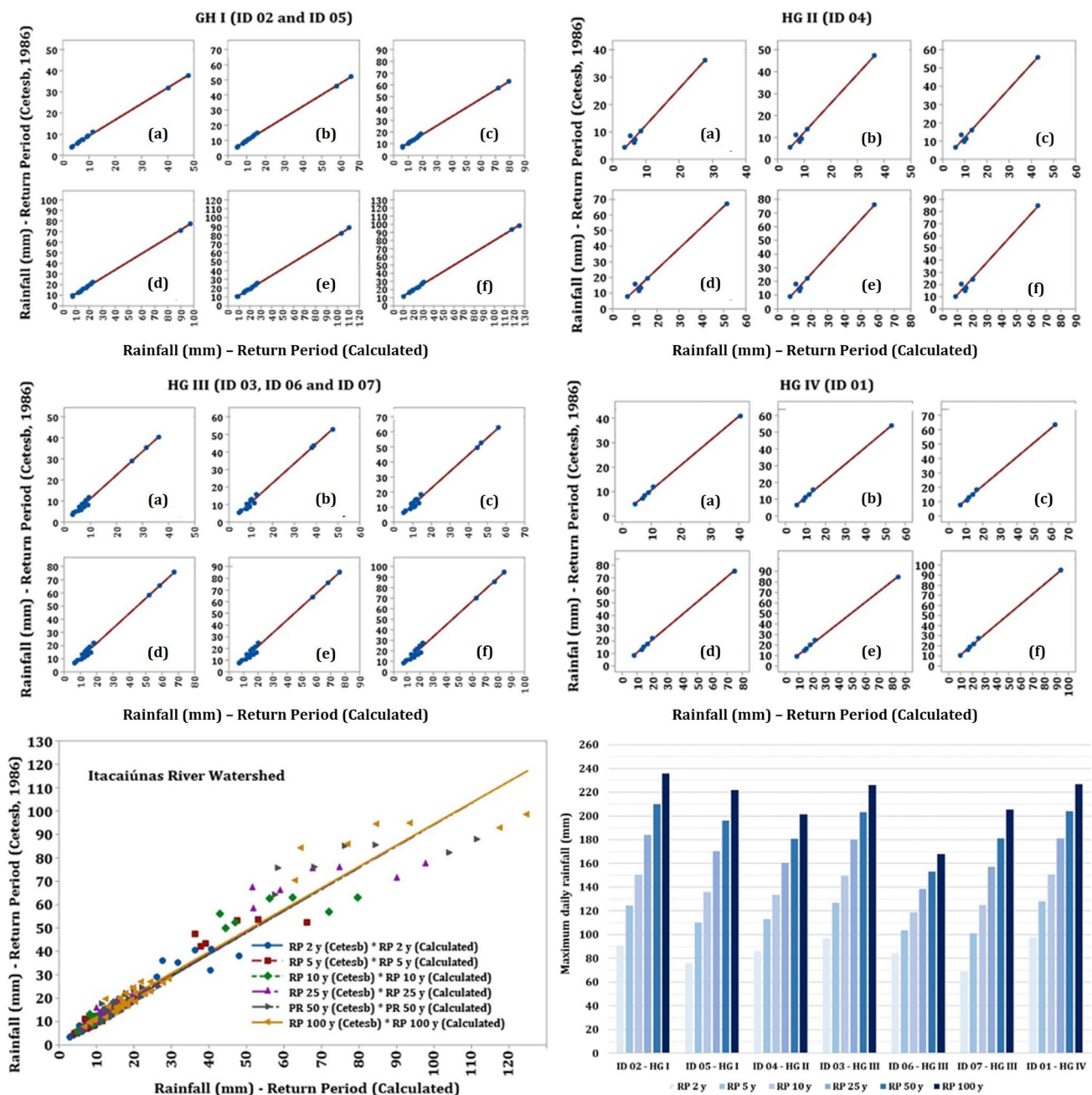
Fig. 5 Scatter graph of maximum hourly rainfall and different return periods estimated from the disaggregation coefficients developed by CETESB (1986) and calculated by this research and the maximum daily rainfall (mm) for different return periods estimated at rain gauges at the weather station in the IRW. The return period of 2 (in **a**), 5 (in **b**), 10 (in **c**), 25 (in **d**), 50 (in **e**), and 100 years (in **f**)

hydraulic works by indicating essential parameters that may prevent or minimize the socioenvironmental impacts of floods and landslides. Future studies should investigate the occurrence of intense rainfall in different climate scenarios, considering the Intergovernmental Panel on Climate Change (IPCC) reports, and examine how the IDF curves would change under these scenarios.

For public managers, we recommend maintaining and improving an active pluviograph station network to measure and understand subdaily extreme events, which is of great relevance to understanding watersheds that have high erosivity levels and dense drainage networks. This information will subsidize the management of risks and vulnerabilities in complex watersheds of interaction between the

Table 7 Intensity-duration-frequency (IDF) (mm h^{-1}) for different return periods (RPs) at rain gauges and weather stations in the homogeneous groups (HGs) in the IRW

D (min)	RP 2 y	RP 5 y	RP 10 y	RP 25 y	RP 50 y	RP 100 y
ID 02—GH-I						
60	48.0	66.0	79.7	97.7	111.3	125.0
360	11.3	15.6	18.8	23.0	26.3	29.5
480	9.4	12.9	15.6	19.1	21.7	24.4
600	7.5	10.3	12.4	15.2	17.3	19.4
720	6.4	8.8	10.7	13.1	14.9	16.7
1440	3.8	5.2	6.3	7.7	8.8	9.8
ID 05—GH-I						
60	40.3	58.4	72.1	90.2	103.9	117.6
360	9.5	13.8	17.0	21.3	24.5	27.7
480	7.9	11.4	14.1	17.6	20.3	23.0
600	6.3	9.1	11.2	14.0	16.2	18.3
720	5.4	7.8	9.6	12.1	13.9	15.7
1440	3.2	4.6	5.7	7.1	8.2	9.2
ID 04—GH-II						
60	27.7	36.4	42.9	51.6	58.1	64.7
360	8.5	11.2	13.2	15.9	17.9	19.9
480	5.3	7.0	8.3	9.9	11.2	12.5
600	6.7	8.8	10.4	12.5	14.1	15.7
720	6.3	8.3	9.8	11.7	13.2	14.7
1440	3.6	4.7	5.6	6.7	7.5	8.4
ID 03—GH-III						
60	36.2	47.6	56.2	67.6	76.2	84.8
360	9.4	12.3	14.5	17.5	19.7	21.9
480	7.6	10.0	11.8	14.2	16.0	17.9
600	8.7	11.4	13.5	16.2	18.3	20.4
720	7.2	9.4	11.1	13.4	15.1	16.8
1440	4.0	5.3	6.2	7.5	8.5	9.4
ID 06—GH-III						
60	31.6	39.0	44.5	51.9	57.5	63.1
360	8.2	10.1	11.5	13.4	14.9	16.3
480	6.7	8.2	9.4	10.9	12.1	13.3
600	7.6	9.4	10.7	12.5	13.8	15.2
720	6.3	7.7	8.8	10.3	11.4	12.5
1440	3.5	4.3	4.9	5.8	6.4	7.0
ID 07—GH-III						
60	25.9	37.9	47.0	58.9	68.0	77.0
360	6.7	9.8	12.1	15.2	17.6	19.9
480	5.5	8.0	9.9	12.4	14.3	16.2
600	6.2	9.1	11.3	14.2	16.3	18.5
720	5.1	7.5	9.3	11.7	13.5	15.3
1440	2.9	4.2	5.2	6.5	7.5	8.6
ID 01—GH-IV						
60	40.5	53.0	62.4	74.9	84.4	93.8
360	10.6	13.8	16.3	19.6	22.0	24.5
480	8.9	11.6	13.7	16.4	18.4	20.5
600	7.4	9.6	11.4	13.6	15.4	17.1
720	6.8	8.9	10.4	12.5	14.1	15.7
1440	4.1	5.3	6.3	7.5	8.5	9.4

natural attributes of the landscape and different land use and types of occupation.

Author contribution Conceptualization, P. M. B. T. and P. R. M.; methodology, P. M. B. T., P. R. M. P, R. L. C., A. C. F. X., and E. A. d. O.; formal analysis, P. M. B. T., P. R. M. P, B. S. S., J. F. O. J.; investigation, P. M. B. T., P. R. M. P, R. L. C., A. C. F. X., J. F. O. J., E. A. d. O. S, B. S., J. B., and A. M. Q. M.; resources, P. M. B. T. and P. R. M.; data curation, P. M. B. T., P. R. M. P, A. C. F. X., B. S. S., and J. F. O. J.; writing (original draft preparation), P. M. B. T. and P. R. M.; writing (review and editing), P. M. B. T., P. R. M. P., R. L. C., A. C. F. X., B. S. S., E. A. d. O. S, J. F. O. J, J. B., A. M. Q. M; visualization, P. M. B. T., B. S., S.; translation, B. S., S; supervision, P. R. M. P. and R. L. C; project administration, P. R. M. P.; funding acquisition, P. R. M. P. All authors have read and approved the manuscript and agree with the authorship order.

Data Availability Not applicable.

Code availability Not applicable.

Declarations

Ethics approval Not applicable.

Consent to participate Not applicable.

Consent for publication All authors have read and agreed to the published version of the manuscript.

Conflict of interest The authors declare no competing interests.

References

Abreu MC, Cecílio RA, Pruski FF, Santos GR, Almeida LT, Zanetti SS, Rodrigues G (2018) Critérios para escolha de distribuições de probabilidades em estudos de eventos extremos de precipitação. Rev Brasil Meteorol 33(4):601–613. https://doi.org/10.1590/0102-7786334004

Abreu MC, Pereira SB, Cecílio RA, Pruski FF, Almeida LT, Silva DD (2022) Assessing the application of ratios between daily and sub-daily extreme rainfall as disaggregation coefficients. Phys Chem Earth, Parts A/B/C 128:103223. https://doi.org/10.1016/j.pce.2022.103223

Alam MA, Emura K, Farnham C, Yuan J (2018) Best-fit probability distributions and return periods for maximum monthly rainfall in Bangladesh. Climate 6(9):1–16. https://doi.org/10.3390/cli6010009

Alcântara CR, Dias MAS, Souza EP, Cohen JC (2011) Verification of the role of the low-level jets in amazon squall lines. Atmos Res 100(1):36–44. https://doi.org/10.1016/j.atmosres.2010.12.023

Almeida CT, Oliveira-Júnior JF, Delgada RC, Cubo P, Ramos MC (2017) Spatiotemporal rainfall and temperature trends throughout the Brazilian Legal Amazon, 1973-2013. Int J Climatol 37(4):2013–2026. https://doi.org/10.1002/joc.4831

Álvares CA, Stape JL, Sentelhas PC, De Moraes Gonçalves JL, Sparovek G (2013) Köppen's climate classification map for Brazil. Meteorol Z 22(6):711–1728. https://doi.org/10.1127/0941-2948/2013/0507

ANA (Agência Nacional das Águas). HIDROWEB (2021) Available in: http://www.snirh.gov.br/hidroweb/publico/medicoes_historicas_abas.jsf). Accessed 29 Mar 2021

Back AJ, Wildner LP (2021) Equação de chuvas intensas por desagregação de precipitação máxima diária para o estado de Santa Catarina. Agro Catarinense 34(3):43–47. https://doi.org/10.52945/rac.v34i3.1133

Beskow S, Caldeira TL, Mello CR, Faria LC, Guedes HAS (2015) Multi-parameter probability distributions for heavy rainfall modeling in Extreme Southern Brazil. Reg Stud 4:123–133. https://doi.org/10.1016/j.ejrh.2015.06.007

Blain GC, Sobierajski GR, Xavier ACF, Carvalho JP (2021) Regional frequency analysis applied to extreme rainfall events: evaluating its conceptual assumptions and constructing null distributions. Anais da Acad Brasil Ciências (Online) 93(1):1–19. https://doi.org/10.1590/0001-3765202120190406

Brasil Neto RM, Santos CAG, Silva RM, Santos CAC, Liu Z, Quinn NW (2021) Geospatial cluster analysis of the state, duration and severity of drought over Paraíba State, northeastern Brazil. Sci Total Environ 799:149492. https://doi.org/10.1016/j.scitotenv.2021.149492

Cahill AT (2003) Significance of AIC differences for precipitation intensity distributions. Adv Water Resour 26(4):457–464. https://doi.org/10.1016/S03091708(02)00167-7

Caldeira TL, Beskow S, Mello CR, Vargas MM, Guedes HAS, Faria LC (2015) Daily rainfall disaggregation: an analysis for the Rio Grande do Sul State. Sci Agraria 16:1–21. https://doi.org/10.5380/rsa.v16i3.46320

Carvalho LMV, Jones C, Liebmann B (2002) Extreme precipitation events in Southern South America and large-scale convective patterns in South Atlantic Convergence Zone. J Clim 15(17):2377–2394

Cavalcante RBL, Pontes PRM, Souza Filho PWM, Souza EB (2019a) Opposite effects of climate and land use changes on the annual water balance in the Amazon Arc of Deforestation. Water Resour Res 55(4):3092–3106. https://doi.org/10.1029/2019WR025083

Cavalcante RBL, Pontes PRM, Tedeschi RG, Costa CPW, Ferreira DBS, Souza Filho PWM, Souza E (2019b) Terrestrial water storage and Pacific SST affect the monthly water balance of Itacaiúnas river basin (eastern Amazonia). Int J Climatol 40 (6): 3021-3035. https://doi.org/10.1002/joc.6380

CETESB - Companhia de Tecnologia de Saneamento Ambiental (1986) Drenagem urbana: manual de projeto, 1st edn. DAEE/CETESB, São Paulo, p 466

Cohen JCP, Dias MAFS, Nobre CA (1995) Environmental conditions associated with Amazonian Squall Lines: a case study. Mon Weather Rev 123:3163–3174

Coles SG, Dixon MJ (1999) Likelihood-based inference for extreme value models. Extremes 2(1):5–23. https://doi.org/10.1023/A:1009905222644

Costa CEAS, Blanco CJC, Oliveira-Júnior JF (2020) IDF Curves for future climate Scenarios in the Amazon. J Water Clim Change 11:760–770. https://doi.org/10.2166/wcc.2019.202

Cunderlik JM, Ouarda TB (2006) Regional flood-duration–frequency modeling in the changing environment. J Hydrol 318(1-4):276–291. https://doi.org/10.1016/j.jhydrol.2005.06.020

Dalagnol R, Gramcianinov CB, Crespo NM, Luiz R, Chiquetto JB, Marques MTA, Dolif Neto G, Abreu RC, Li S, Lott FC, Anderson LO, Sparrow S (2021) Extreme rainfall and its impacts in the Brazilian Minas Gerais state in January 2020: Can we blame climate change? Clim Resil Sustain 0:1–15. https://doi.org/10.1002/cli2.15

Diez-Sierra J, del Jesus M (2019) Subdaily rainfall estimation through daily rainfall downscaling using random forests in Spain. Water 11(1):125. https://doi.org/10.3390/w11010125

Fadhel S, Rico-Ramirez MA, Han D (2017) Uncertainty of Intensity-Duration-Frequency (IDF) curves due to varied climate baseline periods. J Hydrol 547(1):600–612. https://doi.org/10.1016/j.jhydrol.2017.02.013

Falck AS, Maggioni V, Tomasella J, Vila DA, Diniz FLR (2015) Propagation of satellite precipitation uncertainties through a distributed hydrologic model: a case study in the Tocantins-Araguaia basin in Brazil. J Hydrol 527:943–957. https://doi.org/10.1016/j.jhydrol.2015.05.042

Ferreira JC, Daniel LA, Tomazela M (2005) Parâmetros para equações mensais de estimativas de precipitação de intensidade máxima para o Estado de São Paulo - Fase I. Revista Ciência e Agrotecnologia 29(1175-1187):2005. https://doi.org/10.1590/S1413-70542005000600011

Fischer T, Su B, Yong L, Scholten T (2012) Probability distribution of precipitation extremes for weather index-based insurance in the Zhujiang River Basin, South China. J Hydrometeorol 13(3):1023–1037. https://doi.org/10.1175/JHM-D-11-041.1

Fowler HJ, Lenderink G, Prein AF, Westra S, Allan RP, Ban N, Barbero R, Berg P, Blenkinsop S, Do HX, Guerreiro S, Haerter JO, Kendon EJ, Lewis E, Schaer C, Sharma A, Villarini G, Wasko C, Zhang X (2021) Anthropogenic intensification of short-duration rainfall extremes. Nat Rev Earth Environ 2(2):107–122. https://doi.org/10.1038/s43017-020-00128-6

Frich P, Alexander LV, Della-Marta P, Gleason B, Haylock M, Klein Tank AMG, Peterson T (2002) Observed coherent changes in climatic extremes during the second half of the twentieth century. Clim Res 19(3):193–212

Ghiaei F, Kankal M, Anilan T, Yuksek O (2018) Regional intensity-duration-frequency analysis in the Eastern Black Sea Basin, Turkey, by using L-moments and regression analysis. Theor Appl Climatol 131(1-2):245–257. https://doi.org/10.1007/s00704-016-1953-0

Hastenrath S, Geischar L (1993) Further work of Northeast Brazil rainfall anomalies. J Clim 6(4):743–758

IBGE 2021 (Instituto Brasileiro de Geografia e Estatística). Cidades@. Available in: https://cidades.ibge.gov.br/brasil/pa/panorama. Accessed 25 Aug 2021

INMET (Instituto Nacional de Meteorologia). BDMEP (Banco de Dados Meteorológicos para Ensino e Pesquisa) (2021) Available in: < http://www.inmet.gov.br/portal/index.php?r=bdmep/bdmep >. Accessed 18 June 2021

ITV (Vale Institute of Technology/Sustainable Development). Estações Hidrometeorológicas (EHM) (2021) Available in: https://ehm.itvds.org/. Accessed 18 June 2021

Katz RW (2010) Statistics of extremes in climate change Climatic Change 100(1):71–76. https://doi.org/10.1007/s10584-010-9834-5

Kim H, Kim S, Shin H, Heo JH (2017) Appropriate model selection methods for nonstationary generalized extreme value models. J Hydrol 547:557–574. https://doi.org/10.1016/j.jhydrol.2017.02.005

Koutsoyiannis DK, Kozonis D, Manetas A (1998) A mathematical framework for studying rainfall Intensity-Duration-Frequency relationships. J Hydrol 206(1-2):118–135. https://doi.org/10.1016/S0022-1694(98)00097-3

Koutsoyiannis DK (2003) Rainfall disaggregation methods: theory and applications. In: Piccolo D, Ubertini L (eds) Proceedings, Workshop on Statistical and Mathematical Methods for Hydrological Analysis. Università di Roma "La Sapienza", pp 1–23. https://doi.org/10.13140/RG.2.1.2840.8564

Kunkel KE, Karl TR, Easterling DR, Redmond K, Young J, Yin X, Hennon P (2013) Probable maximum precipitation and climate change. Geophys Res Lett 40(7):1402–1408. https://doi.org/10.1002/grl.50334

Lima AO, Lyra GB, Abreu MC, Oliveira-Júnior JF, Zeri M, Cunha-Zeri G (2021) Extreme rainfall events over Rio de Janeiro State, Brazil: characterization using probability distribution functions and clustering analysis. Atmos Res 247:1–17. https://doi.org/10.1016/j.atmosres.2020.105221

Lima MG, Santana DC, Maciel Junior IC, Costa PMC, Oliveira PPG, Azevedo RP, Silva RS, Marinha UF, Silva V, Souza JAA, Rossi FS, Delgado RC, Teodoro LP, Teodoro PE, Silva Junior CA (2022) The "New Transamazonian Highway": BR-319 and its current environmental degradation. Sustainability 14(2):823. https://doi.org/10.3390/su14020823

Marengo JA (2005) Characteristics and spatial-temporal variability of the Amazon River Basin water budget. Clim Dyn 24(1):11–22. https://doi.org/10.1007/s00382004-0461-6

Martins D, Gandini MLT, Kruk NS, Queiroz PIV (2019) Disaggregation of daily rainfall data for the Caraguatatuba city, in São Paulo State. Brazil Brazilian J Water Resour 24(39):1–8. https://doi.org/10.1590/2318-0331.241920180100

Merz B, Aerts J, Arnbjerg-Nielsen K, Baldi M, Becker A, Bichet A, Blöschl G, Bouwer LM, Brauer A, Cioffi F, Delgado JM, Gocht M, Guzzetti F, Harrigan S, Hirschboeck K, Kilsby C, Kron W, Kwon HH, Lall U et al (2014) Floods and climate: emerging perspectives for flood risk assessment and management. Nat Hazards Earth Syst Sci 14(7):1921–1942. https://doi.org/10.5194/nhess-14-1921-2014

Moccia B, Mineo C, Ridolfi E, Russo F, Napolitano F (2021) Probability distributions of daily rainfall extremes in Lazio and Sicily, Italy, and design rainfall inferences. J Hydrol Reg Stud 33(2021):100771. https://doi.org/10.1016/j.ejrh.202

Mohymont BG, Demarée GR, Faka DN (2004) Establishment of IDF-Curves for precipitation in the tropical area of Central Africa. Nat Hazards Earth Syst Sci 4(3):375–387. https://doi.org/10.5194/nhess-4-375-2004

Morabbi A, Bouziane A, Seidoub O, Habitou N, Ouazar D, Ouarda TBMJ, Charron C, Hasnaoui MD, Benrhanem M, Sittichokg K (2022) A multiple changepoint approach to hydrological regions delineation. J Hydrol 604(2022):127118. https://doi.org/10.1016/j.jhydrol.2021.127118

Navares R, Aznarte JL (2020) Forecasting Plantago pollen: improving feature selection through random forests, clustering, and Friedman tests. Theor Appl Climatol 139(4):163–174. https://doi.org/10.1007/s00704-019-02954-1

Nobre CA, Sellers P, Shukla J (1991) Amazonian deforestation and regional climate change. J Clim 4(10):957–988. https://doi.org/10.1175/1520-0442(1991)004<0957:ADARCC>2.0.CO;2

Nunes S, Cavalcante RBL, Nascimento WR, Souza-Filho PWM, Santos D (2019) Potential for forest restoration and deficit compensation in Itacaiúnas Watershed. Southeastern Brazil Amazon Forests 10(5):439. https://doi.org/10.3390/f10050439

Oliveira LFC, Antonini JC, Griebeler N (2008) Métodos de estimativa de precipitação máxima para o estado de Goiás. Rev Brasil Engenharia Agrícola e Ambiental 12(6):620–625. https://doi.org/10.1590/S1415-43662008000600008

Passos MLV, Mendes TJ (2018) Análise de eventos pluviométricos extremos no município de Balsas - MA. Caminhos de Geografia 19(66):85–96. https://doi.org/10.14393/RCG196606

Passos JBMC, Silva DD, Lima RRPC (2021) Daily rainfall disaggregation coefficients for the Doce river basin, Brazil: Regional applicability and the Return Period influence. Engenharia Agrícola 41(2):223–234. https://doi.org/10.1590/1809-4430-Eng.Agric.v41n2p223-234/2021

Papalexiou SM, Koutsoyiannis D, Makropoulos C (2013) Extreme is extreme? An assessment of daily rainfall distribution tails. Hydrol Earth Syst Sci 17(2):851–862. https://doi.org/10.5194/hess-17-851-2013

Pui A, Sharma A, Mehrotra R, Sivakumar B, Jeremiah E (2012) A comparison of alternatives for daily to sub-daily rainfall disaggregation. J Hydrol 470-471:138–157. https://doi.org/10.1016/j.jhydrol.2012.08.041

Rulfová Z, Buishand TA, Roth M, Kysely J (2016) A two-component generalized ex-treme value distribution for precipitation frequency analysis. J Hydrol 534:659–668. https://doi.org/10.1016/j.jhydrol.2016.01.032

Sane Y, Panthou G, Bodian A, Vischel T, Lebel T, Dacosta H, Quantin G, Wilcox C, Ndiaye O, Diongue-Niang A, Diop KM (2018) Intensity–duration–frequency (IDF) rainfall curves in Senegal. Nat Hazards Earth Syst Sci 18(7):1849–1866. https://doi.org/10.5194/nhess-18-1849-2018

Santos EB, Lucio PS, Silva CMS (2015) Seasonal analysis of return periods for maximum daily precipitation in the Brazilian Amazon. J Hydrometeorol 16(3):973–984. https://doi.org/10.1175/JHM-D-14-0201.1

Santos CAG, Brasil Neto RM, Silva RM, Costa SGF (2019a) Cluster analysis applied to spatiotemporal variability of monthly precipitation over Paraíba state using Tropical Rainfall Measuring Mission (TRMM) Data. Remote Sens 11(6):637. https://doi.org/10.3390/rs11060637

Santos V, Blanco CJC, Oliveira Júnior JF (2019b) Distribution of rainfall probability in the Tapajós river basin, Amazonia. Brazil Revista Ambiente e Água 14(3):1–21. https://doi.org/10.4136/ambi-agua.2284

Serrão EAO, Silva MT, Ferreira TR, Ataide LCP, Wanzeler RTS, Silva VPR, Lima AMM, Sousa FAS (2021) Large-Scale hydrological modeling of flow and hydropower production, in a Brazilian watershed. Ecohydrol Hydrobiol 21(1):23–35. https://doi.org/10.1016/j.ecohyd.2020.09.002

Shiau JT, Lin JW (2016) Clustering quantile regression-based drought trends in Taiwan. Water Resour Manag 30(3):105–1069. https://doi.org/10.1007/s11269-015-1210-9

Silva DF, Simonovic SP, Schardong A, Goldenfum JA (2021) Introducing Non-Stationarity into the development of intensity-duration-frequency curves under a chan-ging climate. Water 13(8):1008. https://doi.org/10.3390/w13081008

Silva Cruz J, Blanco CJC, Oliveira Júnior JF (2022) Modeling of land use and land cover change dynamics for future projection of the Amazon number curve. Sci Total Environ 811:152348. https://doi.org/10.1016/j.scitotenv.2021.152348

Silva Júnior CA, Costa GM, Rossi FS, Vale JCE, Lima RB, Lima M, Oliveira-Júnior JF, Teodoro PE, Santos RC (2019) Remote sensing for updating the boundaries between the brazilian Cerrado-Amazonia Biomes. Environ Sci Pol 101:383–392. https://doi.org/10.1016/j.envsci.2019.04.006

Silva Júnior CA, Lima MG, Teodoro P, Oliveira-Júnior JF, Rossi FS, Funatsu BM, Butturi W, Lourenconi T, Kraeski A, Pelissari TD, Moratelli FA, Arvor D, Luz IMS, Teodoro LPR, Dubreuil V, Teixeira VM (2022) Fires drive long-term environmental degradation in the Amazon Basin. Remote Sens 14(2):338. https://doi.org/10.3390/rs14020338

Silva Neto VL, Viola MR, Silva DD, Mello CR, Pereira SB, Giongo M (2017) Daily rainfall disaggregation for Tocantins State Brazil. Revista Ambiente & Água 12(4):605–617. https://doi.org/10.4136/ambi-agua.2077

Silva Neto VL, Viola MR, Mello CR, Alves MVG, Silva DD, Pereira SB (2020) Mapeamento de chuvas intensas para o estado do Tocantins. Revista Brasileira de Meteorologia 35(1):1–11. https://doi.org/10.1590/0102-7786351017

Silva Neto VL, Viola MR, Morais MAV, Cardoso JAF, Silva Lima IC, Ferreira WB (2021) Desagregação de chuva diária para o estado da Bahia, Brasil. Res , Soc Dev 10(16):e197101623513. https://doi.org/10.33448/rsd-v10i16.23513

Silveira ALL (2000) Equação para os coeficientes de desagregação da chuva. Rev Bras Recur Hidr 5(4):143–147

Souza-Filho PWM, Nascimento WR, Santos DC, Weber EJ, Silva RO, Siqueira JO (2018) A GEOBIA approach for multitemporal land-cover and land-use change analysis in a tropical watershed in the southeastern Amazon. Remote Sens 10:1683. https://doi.org/10.3390/rs10111683

Svensson C, Clarke RT, Jones DA (2007) An experimental comparison of methods for estimating rainfall intensity-duration-frequency relations from fragmentary records. J Hydrol 341(1-2):79–89. https://doi.org/10.1016/j.jhydrol.2007.05.002

Svensson C, Jones DA (2010) Review of rainfall frequency estimation methods. J Flood Risk Manag 3(4):296–313. https://doi.org/10.1111/j.1753-318X.2010.01079.x

Tabari H (2020) Climate change impact on flood and extreme precipitation increases with water availability. Sci Rep 10:13768. https://doi.org/10.1038/s41598-02070816-2

Tavares AL, Carmo AMC, Silva Júnior RO, Souza-Filho PWM, Silva MS, Ferreira DBS, Nascimento Junior WR, Dall'Agnol R. (2018) Climate indicators for a watershed in the eastern Amazon. Revista Brasileira de Climatologia 23:389–410. https://doi.org/10.5380/abclima.v23i0.61160

Teodoro PE, Oliveira-Júnior JF, Cunha ER, CCG C, Torres FE, Bacani VM, Gois G, Ribeiro LP (2016) Cluster analysis applied to the spatial and temporal variability of monthly rainfall in Mato Grosso do Sul State. Brazil Meteorol Atmos Phys 128(6):197–209. https://doi.org/10.1007/s00703-015-0408-y

Terassi PMB, Oliveira-Júnior JF, Gois G, Oscar-Júnior AC, Sobral BS, Biffi VHR, Blanco CJC, Correia Filho WLF, Vijith H (2020) Rainfall and erosivity in the municipality of Rio de Janeiro-Brazil. Urban Clim 33:100637. https://doi.org/10.1016/j.uclim.2020.100637

Ward JH (1963) Hierarquical grouping to optimize an objective function. J Am Stat Assoc 58(301):236–244. https://doi.org/10.1080/01621459.1963.10500845

Xavier ACF, Rudke AP, Fujita T, Blain GC, Morais MVB, Almeida DS, Raffee SAA, Martins LD, Souza RAF, Freitas ED, Martins JA (2019a) Stationary and nonstationary detection of extreme precipitation events and trends of average precipitation from 1980 to 2010 in the Paraná River basin. Brazil Int J Climatol 40(2):1197–1212. https://doi.org/10.1002/joc.6265

Xavier ACF, Blain GC, Morais MVB, Sobierajski G (2019b) Selecting "the best" nonstationary Generalized Extreme Value (GEV) distribution: on the influence of different numbers of GEV-models.

Bragantia 78(4):606–621. https://doi.org/10.1590/1678-4499.20180408

Xavier, ACF, Rudke AP, Serrão, EAO, Terassi, PMB, Pontes PRM (2021) Evaluation of satellite-derived products for the daily average and extreme rainfall in the mearim river drainage basin (Maranhão Brazil). Remote Sensing 13(21):4393. https://doi.org/10.3390/rs13214393

Ximenes PSMP, Silva ASA, Ashkar F, Stosic T (2021) Best-fit probability distribution models for monthly rainfall of Northeastern Brazil. Water Sci Technol 84(6):1541–1556. https://doi.org/10.2166/wst.2021.304

Yang P, Xia J, Zhang Y, Han J, Wu X (2017) Quantile regression and clustering analysis of standardized precipitation index in the Tarim River Basin, Xinjiang China. Theor Appl Climatol 134(3-4):1–12. https://doi.org/10.1007/s00704-017-2313-4

Ye L, Hanson LS, Ding P, Wang D, Vogel RM (2018) The probability distribution of daily precipitation at the point and catchment scales in the United States. Hydrol Earth Syst Sci 22(12):6519–6531. https://doi.org/10.5194/hess-22-6519-2018

Yilmaz AG, Hossain I, Perera BJC (2014) Effect of climate change and variability on extreme rainfall intensity–frequency–duration relationships: a case study of Melbourne. Hydrol Earth Syst Sci 18:4065–4076. https://doi.org/10.5194/hess-18-4065-2014

Yilmaz AG, Perera C (2015) Spatiotemporal trend analysis of extreme rainfall events in Victoria. Australia Water Resour Manag 29(12):4465–4480. https://doi.org/10.1007/s11269-015-1070-3

Yilmaz AG (2017) Climate change effects and extreme rainfall non-stationarity. Water Manag 170(2):57–65. https://doi.org/10.1680/jwama.15.00049

Yilmaz AG, Imteaz MA, Perera C (2017) Investigation of non-stationarity of extreme rainfalls and spatial variability of rainfall intensity-frequency-duration relationships: A case study of Victoria. Australia Int J Climatol 37(1):430–442. https://doi.org/10.1002/joc.4716

Yuan J, Emura K, Farnham C, Alam MA (2018) Frequency analysis of annual maximum hourly precipitation and determination of best fit probability distribution for regions in Japan. Urban Clim 24:276–286. https://doi.org/10.1016/j.uclim.2017.07.008

Zalina MD, Desa MNM, Nguyen VTA, Kassim AHM (2002) Selecting a probability distribution for extreme rainfall series in Malaysia. Water Sci Technol 45(2):63–68. https://doi.org/10.2166/wst.2002.0028

Zerouali B, Chettih M, Abda Z, Mesbah M, Santos CAG, Brasil Neto RM (2022) A new regionalization of rainfall patterns based on wavelet transform information and hierarchical cluster analysis in northeastern Algeria. Theor Appl Climatol 147(1-2):1–22. https://doi.org/10.1007/s00704-021-03883-8

The manuscript titled "Extreme events and intensity-duration-frequency relationships of rainfall for the Itacaiúnas watershed in the eastern Amazon, Brazil" is original and has not been previously published or is currently under consideration for publication elsewhere.